JOC The Journal of Organic Chemistry

Article

pubs.acs.org/joc

The Inverse Demand Oxa-Diels–Alder Reaction of Resorcinarenes: An Experimental and Theoretical Analysis of Regioselectivity and Diastereoselectivity

Karolina Stefańska,[†] Hanna Jędrzejewska,[‡] Michał Wierzbicki,[‡] Agnieszka Szumna,*[,‡] and Waldemar Iwanek*[,†]

[†]Faculty of Mathematics and Natural Science, The Jan Kochanowski University in Kielce, Świętokrzyska 15, 25-406 Kielce, Poland

[‡]Institute of Organic Chemistry, Polish Academy of Sciences, Kasprzaka 44/52, 01-224 Warsaw, Poland

Supporting Information

ABSTRACT: The Diels–Alder reaction enables introduction of new functionalities onto the resorcinarene skeleton with simultaneous generation of new stereogenic centers and expansion of the internal cavity. We present highly regio- and diastereoselective inverse electron demand oxa-Diels–Alder reactions of resorcinarene *ortho*-quinone methide with benzofuran and indene, each generating 12 new stereogenic centers. The mechanism and reasons for regioselectivity and diastereoselectivity were analyzed using theoretical calculations (NBO charges, Fukui functions, transition state energies, and thermodynamic stability of the products). Enantiomers were separated, and their configurations were determined by comparison of experimental and theoretical electronic circular dichroism spectra.

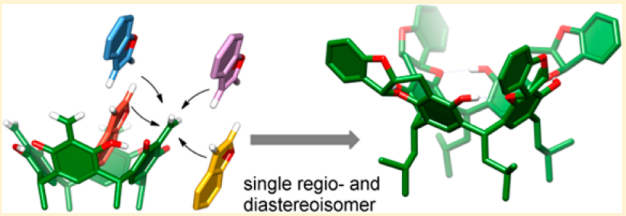

The mainstream research in supramolecular chemistry relies on easily available macrocyclic building blocks that enable a buildup of functional groups on their semirigid scaffolds. Among easily available macrocyclic blocks, resorcinarenes play a relevant role. In their native or functionalized forms, they are used as scaffolds for construction of receptors,[1] cavitands,[2] and capsules[3] for various purposes, including sensing,[4] storage,[5] reaction nanovessels,[6] and biological applications.[7] The possibility of using the Diels–Alder reaction to introduce new functionalities onto the resorcinarene skeleton remained unnoticed until very recently,[8] despite the fact that the potential of this approach is broad. The Diels–Alder reaction is one of the most widely studied and useful reactions for formation of carbon–carbon bonds as well as a powerful method for generation of new stereogenic centers.[9] A great number of substrates and catalysts (including chiral ones) for this reaction is already known. Therefore, the reaction allows the decoration of the resorcinarene core with various groups and can be a valuable method of synthesis of new chiral resorcin[4]arenes. In addition, formation of a six-membered ring expands the internal cavity of the resorcinarene skeleton.[10] Considering the number of reaction sites at the resorcinarene skeleton and the fact that in each event of the Diels–Alder reaction two regioisomers and up to four new stereocenters can be formed, one can easily notice that the stereochemistry of the process can be very advantageous but may also cause serious problems. In the current paper, we present new examples of highly regio- and stereoselective Diels–Alder reactions involving a resorcinarene skeleton and attempt to rationalize the observed stereochemical outcomes of this reaction by means of theoretical calculations.

Recently, we reported a highly regio- and diastereoselective Diels–Alder reaction between a resorcinarene-derived oxadiene and α-methylstyrene (dienophile).[8] The diene component, *ortho*-quinone methide **2**, was thermally generated in situ from **1**, and in the presence of α-methylstyrene, gave a Diels–Alder adduct as a single diastereoisomer in 80% yield. In the current approach, we used benzofuran or indene as dienophiles (Figure 1). We previously found that the temperature of 100–110 °C is required to generate *o*-quinomethine intermediate **2** from resorcinarene **1**. Thus, **1** was subjected to heating in dioxane with 10 equiv of benzofuran **3** or indene **8**. The reaction with **3**, after 24 h, gave a single Diels–Alder product in 74% yield. Longer reaction times did not lead to increased yields: after 48 h the product was obtained in 75% yield and after 5 days in 72% yield. The reaction of **1** with **8** gave a Diels–Alder product in 46% yield. Analysis of the NMR spectra (Figure 2) led to the conclusion that both products were obtained as single diastereoisomers. In principle, for each Diels–Alder reaction site, there are two regioisomers possible (and two diastereoisomers for each regioisomer). Therefore, for four reaction sites, in the most general case, the number of conceivable isomers is very large. However, our NMR data indicate that in both cases we have obtained a single product of C_4 symmetry. Among C_4 symmetric structures, there are four possible isomers (or eight also counting enantiomers, Figure 1 and Figure S1). These are two regioisomers multiplied by two isomers originating from an *endo* or *exo* approach of diene and

Received: May 10, 2016
Published: June 23, 2016

DOI: 10.1021/acs.joc.6b01099
J. Org. Chem. 2016, 81, 6018–6025

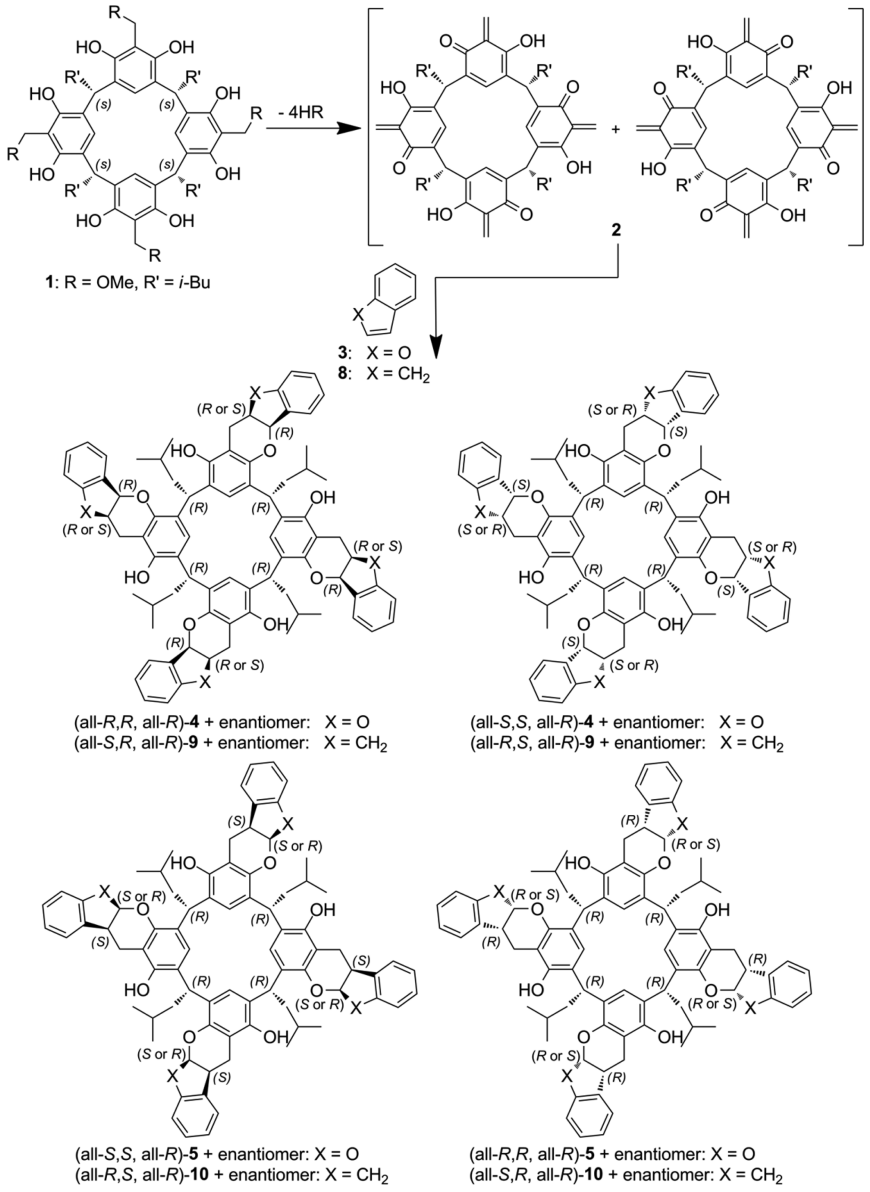

Figure 1. Diels–Alder reaction between benzofuran **3** or indene **8** and *o*-quinomethide resorcinarene **2** and possible C_4 symmetric products (a view from the top (wide rim), all enantiomers are included in the ESI file in Figure S1).

dienophile. Analysis of one-dimensional (1D) and two-dimensional (2D) NMR spectra of the reaction products excludes the formation of regioisomers **5** and **10**. Examination of the ROESY spectra (Figures S5 and S11) indicates that diastereoisomers have (all-*R*,*R*, all-*R*)-**4** and (all-*S*,*R*, all-*R*)-**9** relative configurations. NOEs are observed between *h* protons (at the newly formed stereogenic center) and *a* protons (located in the lower rim alkyl chains). These effects are especially diagnostic because such close contacts are only possible when proton *h* is directed outside the cavity. X-ray structures of **4** and **9** confirm that the obtained diastereoisomers have relative (all-*R*,*R*, all-*R*)-**4** and (all-*S*,*R*, all-*R*)-**9** configurations (Figure 3). In the solid state, (all-*R*,*R*, all-*R*)-**4** and (all-*S*,*R*, all-*R*)-**9** exhibit a cone conformation that is stabilized by four intramolecular hydrogen bonds. Such a hydrogen bonding system is often postulated as a stabilization force for regioselective formation of C_4 symmetric structures. The cavity of the product is quite open, opposite to the previously reported Diels–Alder product with styrene.[8] In the current structures, the cavities are filled with solvent molecules.

Regioselectivity. Rationalization of regioselectivity of this reaction based on simple nonmacrocylic examples is not straightforward. To the best of our knowledge, there are no examples of reactions between *ortho*-quinone methides and benzofuran for direct comparison. *Ortho*-quinone methides are classic examples of electron-poor dienes that are postulated to participate in the Diels–Alder through an inverse demand mechanism (DA_{INV}).[11] In the reaction with highly electron-rich dienophiles such as vinyl ethers, they regioselectively give cyclic acetals (type **5** products), and such regioselectivity is explained based on charge distribution.[12] On the other hand, there is a single literature example of benzofuran participating as a dienophile in the oxa-Diels–Alder reaction, and the resulting regioselectivity was opposite (type **4** products).[13]

To rationalize our experimental results, we performed quantum chemical calculations.[14] We calculated orbitals and their energies for **3**, **7**, and **8** and *o*-quinomethide **6**, being a

DOI: 10.1021/acs.joc.6b01099
J. Org. Chem. 2016, 81, 6018–6025

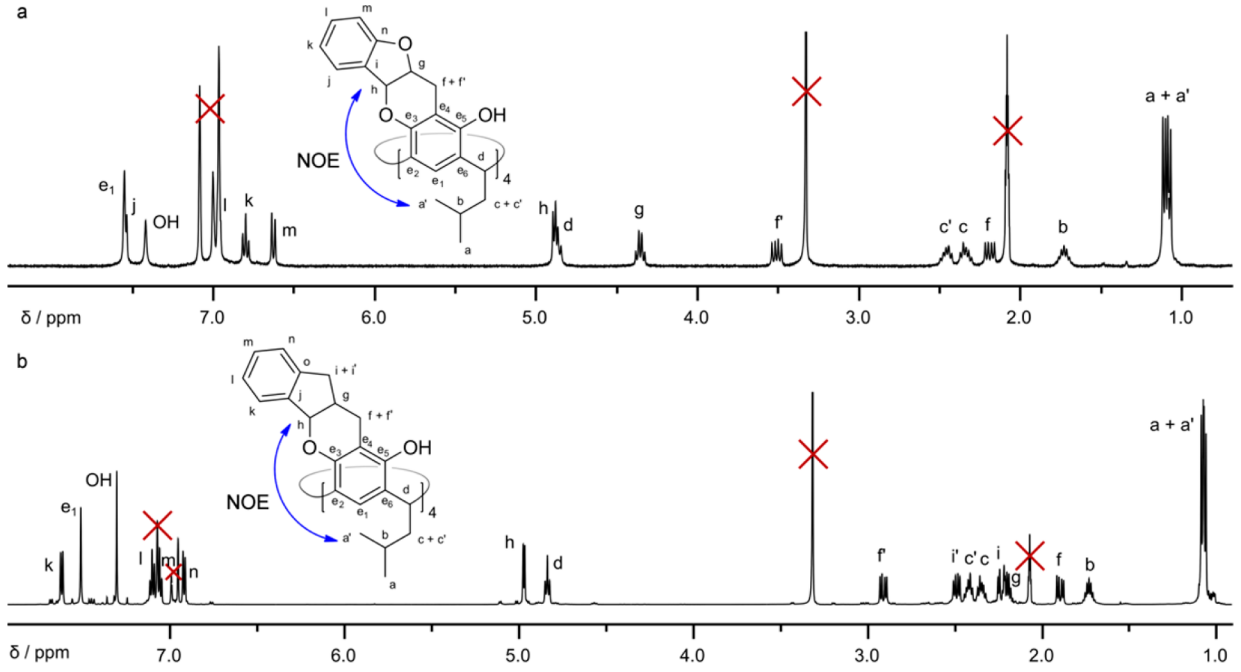

Figure 2. (a) ^{1}H NMR spectrum of **4** (400 MHz, toluene-d_8). (b) ^{1}H NMR spectrum of **9** (600 MHz, toluene-d_8). The signals of 1,4-dioxane and toluene-d_8 have been crossed out.

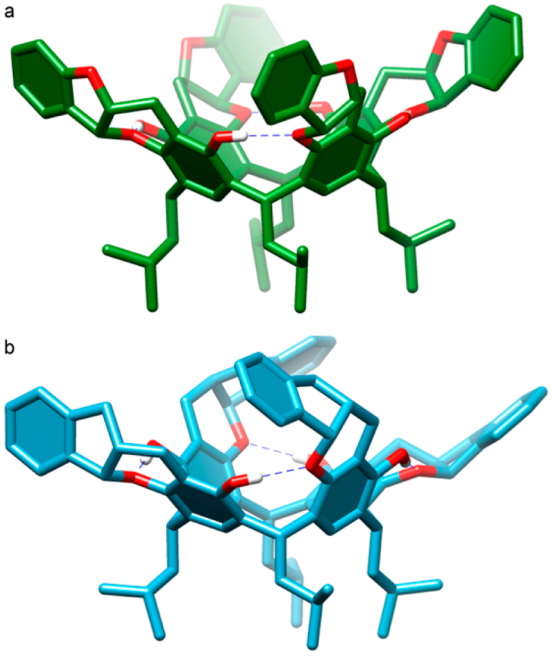

Figure 3. Molecular structure of (a) (all-*R*,*R*, all-*R*)-**4** and (b) (all-*S*,*R*, all-*R*)-**9** determined by X-ray crystallography (CCDC 1470016 and 1483833 respectively). Most hydrogen atoms, guest solvent molecules as well as the second independent molecule of **4** have been omitted for clarity.

simplified model of **2** (Figure 4a). For **3**, **6**, **7**, and **8**, energies and symmetries of HOMO and LUMO orbitals were calculated using four methods: two DFT calculations with different functionals, using MP4, and using an approach that derives HOMO energy from ionization energy and LUMO from electron affinity (Table 1 and Figures 4b–d). The results from all methods are consistent and indicate that, based on the symmetry of the orbitals, the Diels–Alder reaction between substrates is thermally allowed either by the classic mechanism ($HOMO_{diene}$···$LUMO_{dienophile}$) or the inverse electron demand mechanism ($LUMO_{diene}$···$HOMO_{dienophile}$). For all reacting pairs (**6** + **3**, **6** + **7**, and **6** + **8**), smaller energy differences were observed between LUMO of diene **6** and HOMO of dienophiles **3**, **7**, or **8**, which indicates the inverse electron demand Diels–Alder reaction mechanism (all methods).

To explain the regioselectivity of the reaction, charge distributions of diene **6** and dienophiles **3**, **7**, and **8** were calculated using an NBO-based method (natural bond orbital, the method is assumed to give more reliable results than Mulliken charges,[15] which can yield unphysical negative values and strongly depend on the basis set[16] (Figure 4e)). For methylstyrene **7**, the experimentally observed regioselectivity[8] is in agreement with that of the prediction based on calculation of partial charges. For **8**, differences between charges at C2 and C3 are very small. However, for benzofuran **3**, according to partial charges, the reaction should prefer formation of an acetal-type of product, i.e. **5**, which is in disagreement with the experimental results. This discrepancy suggests that the regioselectivity of the DA_{INV} reaction cannot be explained by an electrostatic control mechanism. Another method employable for explaining selectivity in such cases uses reactivity descriptors such as condensed Fukui functions. We calculated the condensed Fukui functions for atoms participating in the formation of new bonds. The calculated functions (using the NBO and MP2 methods,[17] Table 2) show that the C2 atom of the five-membered ring in benzofuran exhibits a greater value of f^- and thus is more reactive toward electrophilic attack than the C3 atom. This is experimentally confirmed by formation of the C2-substituted benzofuran derivatives with electrophilic agents. The relative orbital sizes on individual atoms (Figure 4c) explain the formation of regioisomer **4** because of favorable overlapping of orbitals, maximizing bonding interactions, and minimizing antibonding interactions. The interpretation based on Fukui functions is also in agreement with the observed regioselectivity for methylstyrene **7** and indene **8**. To further

DOI: 10.1021/acs.joc.6b01099
J. Org. Chem. 2016, 81, 6018–6025

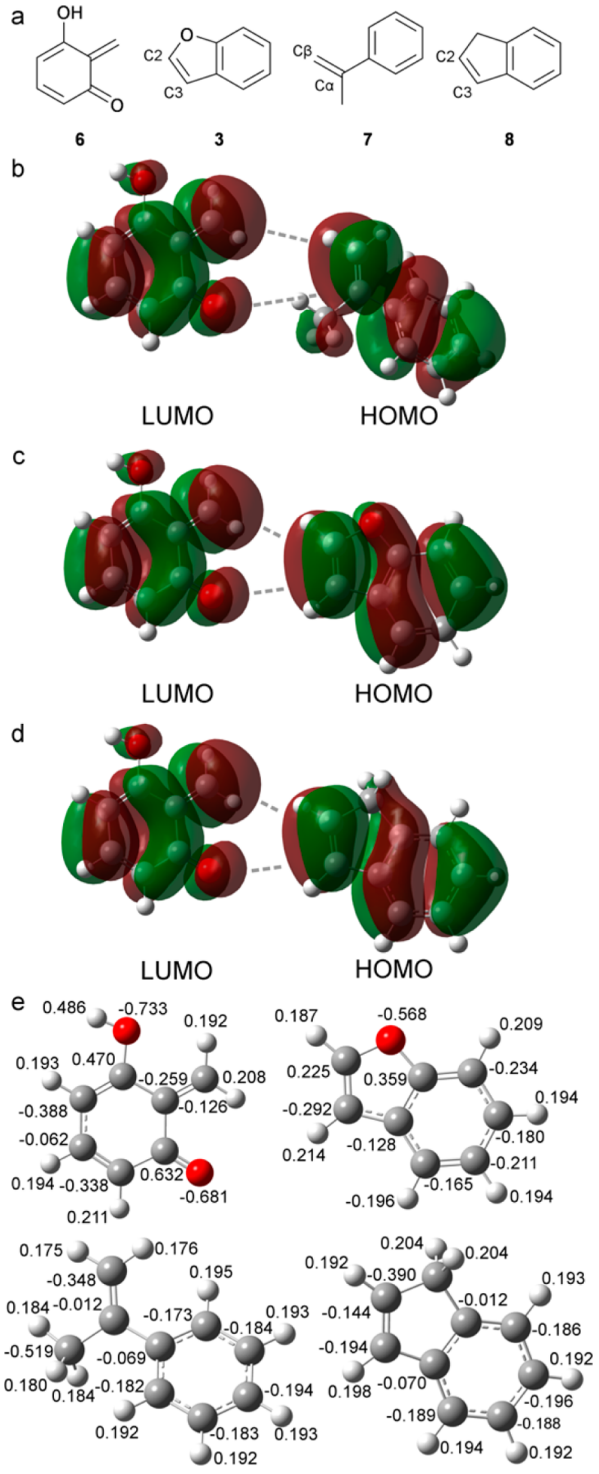

Figure 4. (a) Structures of diene **6** and dienophiles **3**, **7**, and **8** used for the calculations. (b–d) HOMO and LUMO orbitals of **6** and **3** (b), **6** and **7** (c), and **6** and **8** (d) calculated with DFT B3PW91/6-311+g(2d,p) with overlapping orbitals in an inverse electron demand Diels–Alder reaction. (e) Atomic charges in **6**, **3**, **7**, and **8** (NBO, MP2/6-311+g(2d,p)).

support our conclusions based on Fukui functions (especially the equivocal explanation for benzofuran), we have also calculated geometries and energies of transition states for the reactions of **6** + **3** and **6** + **8** using the QST3 approach (DFT B3LYP/631g(d)). Four transition states for each reaction were optimized (two regioisomeric products and two approaches of dienophile, Figure 5). The results confirm that for reaction **6** + **3**, two transition states leading to regioisomers **4** (TS-*endo*-"**4**" and TS-*exo*-"**4**") have energies lower than those in transition states leading to regioisomers **5** (TS-*endo*-"**5**" and TS-*exo*-"**5**"). For reaction **6** + **8**, transition states leading to regioisomers **9** (TS-*endo*-"**9**" and TS-*exo*-"**9**") have energies lower than those in transition states leading to regioisomers **10** (TS-*endo*-"**10**" and TS-*exo*-"**10**"). Both theoretical results are in agreement with experimental results.

Diastereoselectivity. Diastereoselectivity of the reaction of dienophiles with dienes is typically rationalized by an *endo* or *exo* approach. The preference toward an *endo* approach is often observed due to secondary orbital effects, in spite of the fact that *endo* products often have lower thermodynamic stability than *exo* products. In agreement with this common observation, our calculations of transition states for nonmacrocylic analogues **6** and **3** (Figure 5) have confirmed that the *endo* transition state has lower energy, although the difference between TS-*endo*-"4" and TS-*exo*-"4" is rather small.

For macrocyclic compounds, many reactions follow different pathways due to steric reasons. For resorcinarene, experimentally observed (all-*R*,*R*, all-*R*)-**4** must be a result of either an "external"—*exo* approach or a "cavity"—*endo* approach (Figure 6a). We overlaid the calculated transitions states for nonmacrocylic analogues at the resorcinarene skeleton and found that, among these two pathways, the cavity *endo* approach can be hindered due to steric reasons (Figure 6b), and we therefore assume that the observed product is a result of the less-crowded "external"—*exo* approach. The remaining two trajectories are also unfavorable due to steric reasons. The "external"—*endo* approach is due to steric crowding coming from the lower rim alkyl groups (Figure 6c). In the case of the "cavity"—*exo* approach, hindrance may be especially severe at the late stages of the reaction (substitution at the second, third, and fourth ring); however, at the initial stages of the reaction, this approach cannot be excluded. The least-crowded "external"—*exo* approach can also be used for explanation of diastereoselectivity of all other products (all-*S*,*R*, all-*R*)-**9** and a previously observed adduct with methylstyrene **7**.[8]

In addition to the explanation of diastereoselectivity based on possible approach pathways, we also considered relative stability of diastereoisomers. The Diels–Alder reaction is a reversible reaction, and we used rather harsh thermal conditions; therefore, the outcome of the reaction may be thermodynamically controlled and explained by the relative stability of the products. We calculated the energies of all isomers of **4** and **5** presented in Figure 1, each in two conformations arising from flexibility of the pyran ring ("*in*" and "*out*"). We considered only C_4 symmetric conformations; thus, a total of eight initial structures were optimized. The *out* and *in* conformers of (all-*R*,*R*, all-*R*)-**4** after geometry optimization converged to the same structure, very close to the structure observed in the solid state. Indeed, among diastereoisomers of **4**, the experimentally observed isomer (all-*R*,*R*, all-*R*)-**4** has the lowest energy (Figure 7). However, it is important to note that, according to calculations, the regioisomers **5** (not observed experimentally, probably due to electronic requirements as we reasoned above) have energies substantially lower than those of the corresponding regioisomers **4**.

Enantiomers. In the current Diels–Alder reaction, we did not attempt to control enantioselectivity; thus, the obtained products are racemic mixtures of two enantiomers, i.e., (all-*R*,*R* all-*R*)-**4** and (all-*S*,*S* all-*S*)-**4**. The mixture *rac*-(all-*R*,*R* all-*R*)-**4**

DOI: 10.1021/acs.joc.6b01099
J. Org. Chem. 2016, 81, 6018–6025

Table 1. Calculated HOMO and LUMO Energies (eV)

method	**6** HOMO	**6** LUMO	**3** HOMO	**3** LUMO	**7** HOMO	**7** LUMO	**8** HOMO	**8** LUMO
DFT B3LYP/6-311+G(2d,p)	−6.25	−2.93	−6.33	−0.93	−6.38	−1.07	−6.11	−0.91
DFT B3PW91/6-311+G(2d,p)	−6.24	−2.93	−6.36	−0.92	−6.42	−1.07	−6.16	−0.91
HOMO = $E_{neutral} - E_{cation}$ /LUMO = $E_{anion} - E_{neutral}$	−8.01	−1.29	−8.14	0.70	−8.04	0.26	−7.89	−0.65
MP4/6-311+G(2d,p)	−8.45	0.76	−8.28	1.73	−8.45	1.75	−8.01	1.81

Table 2. Calculated Fukui Functions (NBO, MP2/6-311+g(2d,p))

atom	$f^- = q_A(N-1) - q_A(N)$	$f^+ = q_A(N) - q_A(N+1)$
3-C2	0.218	0.168
3-C3	0.074	0.015
6-C	0.169	0.234
6-O	0.247	0.169
7-Cα	0.066	no convergence
7-Cβ	0.251	no convergence
8-C2	0.231	0.002
8-C3	0.054	0.016

was chromatographically separated using a chiral column. Due to low solubility, the electronic circular dichroism (ECD) spectra recorded for both separated peaks are poorly shaped. To assign the absolute configuration, quantum-mechanic computations using the TDDFT method were performed for the optimized structure of (all-*R*,*R* all-*R*)-**4** (B3LYP/6-31g(d)). The theoretically calculated spectrum shows a similarity closer to that of the experimental ECD spectrum of the enantiomer with the shorter retention time (Figure 8). Although not all calculated transitions are experimentally observed, we assume that the lowest energy transitions are the most reliable. We previously observed a similar dependence for other inherently chiral resorcin[4]arenes.[18] For (all-*R*,*R* all-*R*)-**4**, the lowest energy band derives from HOMO → LUMO and HOMO → LUMO + 4 transitions. Shapes of the orbitals indicate that the HOMO → LUMO transition involves orbitals localized at resorcinarene and benzofuran parts; thus, it is most diagnostic for the determination of relative stereochemistry of these two groups (Figure 9).

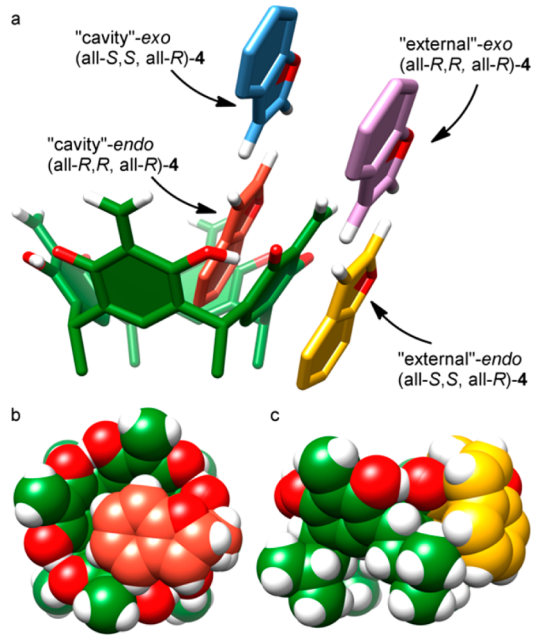

Figure 6. (a) Four possible approaches of dienophile **3** to diene **2**. (b) Steric crowding during the "cavity"—*endo* approach. (c) steric crowding during the "external"—*endo* approach (overlay of optimized structure of **2** and calculated transition states of the reaction between **6** and **3**).

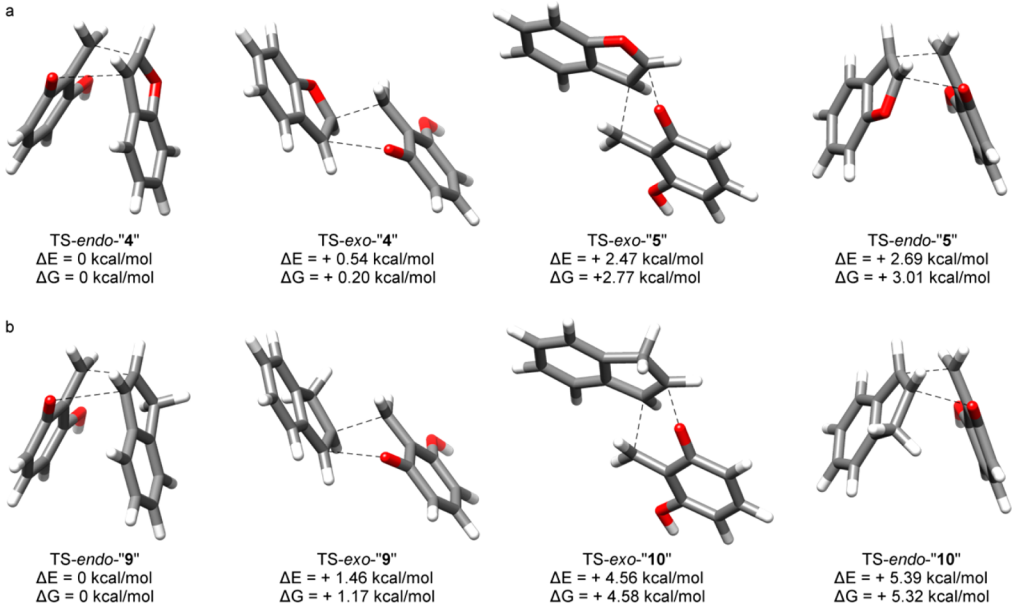

Figure 5. Transition states of reactions between (a) **6** and **3** and (b) **6** and **8** (calculated with QST3, DFT B3LYP/631g(d)).

DOI: 10.1021/acs.joc.6b01099
J. Org. Chem. 2016, 81, 6018−6025

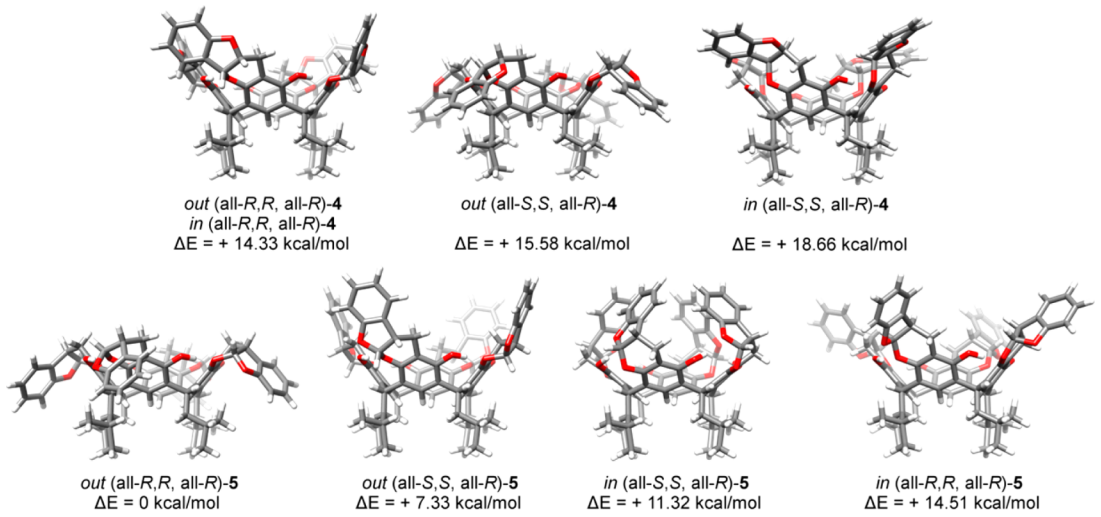

Figure 7. Calculated geometries and energy differences of diastereoisomers of **4** and **5** (calculated with DFT B3LYP/6-31+g(d,p)).

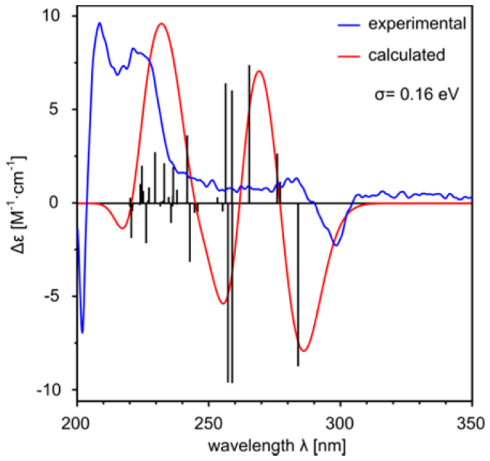

Figure 8. Overlap of the experimental ECD spectrum of the first eluting enantiomer (blue) and the theoretically calculated ECD spectrum for compound **4** (red, scaled by a factor of 1/10 and calculated with TDDFT B3LYP/6-31g(d)).

CONCLUSION

New chiral resorcinarene derivatives were synthesized via an inverse electron demand oxa-Diels–Alder reaction. Resorcinarene *ortho*-quinone methide was thermally generated in situ and subsequently reacted with benzofuran or indene. The reactions between these achiral substrates have the possibility to produce different regioisomers and simultaneously generate 12 new stereogenic centers. However, we show that the reaction proceeds in a highly regio- and diastereoselective way, giving single diastereoisomers (all-*R*,*R*, all-*R*)-**4** or (all-*S*,*R*, all-*R*)-**9** (as racemic mixtures). Theoretical DFT calculations involving analysis of partial charges and Fukui functions of model substrates and transition states allowed us to rationalize experimental regioselectivity. Diastereoselectivity of the reaction was explained based on the steric requirements of *endo* and *exo* approaches between diene and dienophile. Additionally, we showed that the diastereoselectivity of this Diels–Alder reaction is in agreement with the relative thermodynamic stability of the diastereoisomers for the given regioisomer. The enantiomers of chiral resorcinarenes were separated, and their absolute configurations were determined by comparison of experimental and theoretical ECD spectra. We believe that the extended scope of the synthetic strategy and explanation of regio- and diastereoselectivity will trigger application of the Diels–Alder reaction as a new general method of resorcinarene functionalization.

EXPERIMENTAL SECTION

NMR spectra were measured at 400, 500, or 600 MHz. Mass spectra were recorded with the electrospray (ESI) technique and TOF analyzer. The crystal structures were solved with SHELXS and refined with SHELXL. The chromatographic separation of the benzofuran

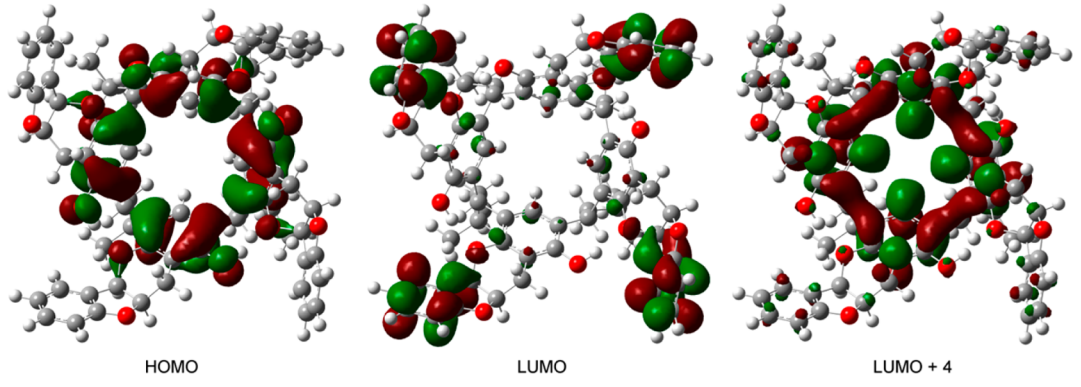

Figure 9. Molecular orbitals of optimized structure of **4**.

DOI: 10.1021/acs.joc.6b01099
J. Org. Chem. 2016, 81, 6018–6025

derivative of resorcinarene **4** into enantiomers was performed using HPLC. Electronic circular dichroism spectra of the obtained fractions were measured using a polarimeter. Reactions were monitored by thin-layer chromatography (TLC) on plastic sheets coated with Kieselgel 60 F254 silica gel. TLC plates were visualized by UV radiation at a wavelength of 254 nm. Reagents and solvents were used without purification.

4: A methoxy derivative of resorcinarene **1** (0.325 mmol, 289 mg), benzofuran **3** (3.25 mmol, 0.36 mL, 10 equiv), and 1,4-dioxane (20 mL) were stirred at 120 °C for 48 h. After being cooled to the room temperature, the precipitate was filtered, washed with 1,4-dioxane, and dried (301 mg, 75% yield). Next, the product (0.244 mmol, 301 mg) was dissolved in a minimum amount of toluene and left to crystallize. Product **4** was obtained in 62% yield (249 mg). White crystals, mp >300 °C (decomposition). ^{1}H NMR (400 MHz, toluene-d$_8$) δ 7.55 (s, 1H, e_1), 7.54 (s, 1H, *j*), 7.42 (s, 1H, *OH*), 6.96−6.94 (m, 1H, *l*), 6.82−6.78 (m, 1H, *k*), 6.63 (d, J = 8.4 Hz, 1H, *m*), 4.89 (d, J = 6.4 Hz, 1H, *h*), 4.87 (t, J = 7.8 Hz, 1H, *d*), 4.35 (ddd, J_1 = 6.4 Hz, J_2 = 8.1 Hz, J_3 = 7.4 Hz, 1H, *g*), 3.51 (dd, J_1 = 8.1 Hz, J_2 = 15.5 Hz, 1H, *f*′), 2.50−2.42 (m, 1H, *c*′), 2.37−2.30 (m, 1H, *c*), 2.19 (dd, J_1 = 7.4 Hz, J_2 = 15.5 Hz, 1H, *f*), 1.77−1.68 (m, 1H, *b*), 1.09 (dd, J_1 = 6.6 Hz, J_2 = 12.6 Hz, 6H, *a* + *a*′). ^{13}C NMR (100 MHz, toluene-d$_8$) δ 160.9 (*n*), 150.2 (e_3 or e_5), 150.1 (e_5 or e_3), 131.4 (*l*), 126.0 (*j*), 124.1 (*i*), 121.1 (e_1), 120.8 (*k*), 112.9 (e_4), 110.7 (*m*), 81.9 (*g*), 80.9 (*h*), 43.6 (*c*), 31.7 (*d*), 26.2 (*b*), 22.9 (*f*), 22.8 (*a*), 22.5 (*a*′). The e_2 and e_6 carbon signals overlap with the residual signals of deuterated toluene, as can be deduced from 2D NMR data. HRMS (ESI) *m*/*z* calcd for $C_{80}H_{80}O_{12}Na$ 1255.5547, found 1255.5582 (|Δ| = 2.8 ppm).

9: A methoxy derivative of resorcinarene **1** (0.325 mmol, 289 mg), indene **8** (3.25 mmol, 0.38 mL, 10 equiv), and 1,4-dioxane (20 mL) were stirred at 120 °C for 72 h. After being cooled to the room temperature, the precipitate was filtered, washed with 1,4-dioxane, and dried (183 mg, 46% yield). White crystals, mp >300 °C (decomposition). ^{1}H NMR (600 MHz, toluene-d$_8$) δ 7.62 (d, J = 7.1 Hz, 1H, *k*), 7.52 (s, 1H, e_1), 7.31 (s, 1H, *OH*), 7.12−7.09 (m, 1H, *l*), 7.07−7.04 (m, 1H, *m*), 6.92 (d, J = 7.4 Hz, 1H, *n*), 4.97 (d, J = 5.8 Hz, 1H, *h*), 4.84 (t, J = 7.9 Hz, 1H, *d*), 2.91 (dd, J_1 = 7.0 Hz, J_2 = 16.3 Hz, 1H, *f*′), 2.49 (dd, J_1 = 7.0 Hz, J_2 = 15.3 Hz, 1H, *i*′), 2.45−2.39 (m, 1H, *c*′), 2.38−2.32 (m, 1H, *c*), 2.23 (dd, J_1 = 6.0 Hz, J_2 = 15.3 Hz, 1H, *i*), 2.22−2.17 (m, 1H, *g*), 1.89 (dd, J_1 = 7.0 Hz, J_2 = 16.3 Hz, *f*), 1.76−1.70 (m, 1H, *b*), 1.07 (dd, J_1 = 6.7 Hz, J_2 = 9.5 Hz, *a* + *a*′). ^{13}C NMR (150 MHz, toluene-d$_8$) δ 150.0 (e_5), 149.8 (e_3), 143.3 (*j*), 141.4 (*o*), 128.8 (*m*), 126.7 (*l*), 125.4 (e_6), 125.3 (*k*), 125.0 (*n*), 124.1 (e_2), 120.8 (e_1), 112.2 (e_4), 82.6 (*h*), 43.9 (*c*), 37.8 (*g*), 36.8 (*i*), 31.5 (*d*), 26.2 (*b*), 22.9 (*a*′), 22.6 (*a*), 22.2 (*f*). HRMS (ESI) *m*/*z* calcd for $C_{84}H_{87}O_8$ 1223.6401, found 1223.6393 (|Δ| = 0.7 ppm).

■ ASSOCIATED CONTENT

Supporting Information

The Supporting Information is available free of charge on the ACS Publications website at DOI: 10.1021/acs.joc.6b01099.

Full spectra of compounds **4** and **9**, chromatography and ECD details, and theoretical calculation details (PDF)
Crystallographic data for **4** (CIF)
Crystallographic data for **9** (CIF)

■ AUTHOR INFORMATION

Corresponding Authors

*E-mail: agnieszka.szumna@icho.edu.pl.
*E-mail: iwanek@ujk.kielce.pl.

Notes

The authors declare no competing financial interest.

■ ACKNOWLEDGMENTS

This work is gratefully dedicated to Prof. Janusz Jurczak on the occasion of his 75th birthday and for his long-standing ample support and many helpful discussions. K.S., M.W., and W.I. acknowledge the financial support of the National Science Centre, Poland (Grant 2012/05/B/ST5/00306). H.J. and A.S. were supported by the Foundation for Polish Science (Grant POMOST/2011-4/10). Calculations were carried out using resources provided by Wroclaw Centre for Networking and Supercomputing (http://wcss.pl, Grant 299).

■ REFERENCES

(1) (a) Matthews, S. E.; Beer, P. D. *Supramol. Chem.* **2005**, *17*, 411−435. (b) Zhu, S. S.; Staats, H.; Brandhorst, K.; Grunenberg, J.; Gruppi, F.; Dalcanale, E.; Lützen, A.; Rissanen, K.; Schalley, C. A. *Angew. Chem., Int. Ed.* **2008**, *47*, 788−792. (c) Murayama, K.; Aoki, K. *Chem. Commun.* **1997**, 119−120.

(2) (a) Gibb, C. L. D.; Gibb, B. C. *J. Am. Chem. Soc.* **2004**, *126*, 11408−11409. (b) Leigh, D. A.; Linnane, P.; Pritchard, R. G.; Jackson, G. *J. Chem. Soc., Chem. Commun.* **1994**, 389−390. (c) Barrett, E. S.; Irwin, J. L.; Edwards, A. J.; Sherburn, M. S. *J. Am. Chem. Soc.* **2004**, *126*, 16747−16749. (d) Pochorovski, I.; Ebert, M.-O.; Gisselbrecht, J.-P.; Boudon, C.; Schweizer, W. B.; Diederich, F. *J. Am. Chem. Soc.* **2012**, *134*, 14702−14705.

(3) (a) MacGillivray, L. R.; Atwood, J. L. *Nature* **1997**, *389*, 469−472. (b) Shivanyuk, A.; Rebek, J., Jr. *J. Am. Chem. Soc.* **2003**, *125*, 3432−3433. (c) Avram, L.; Cohen, Y. *Org. Lett.* **2003**, *5*, 3329−3332. (d) Beyeh, N. K.; Kogej, M.; Ahman, A.; Rissanen, K.; Schalley, C. A. *Angew. Chem., Int. Ed.* **2006**, *45*, 5214−5218.

(4) (a) Nikolelis, D. P.; Petropoulou, S.-S. E.; Pergel, E.; Toth, K. *Electroanalysis* **2002**, *14*, 783−790. (b) Dickert, F. L.; Bäumler, U. P. A.; Stathopulos, H. *Anal. Chem.* **1997**, *69*, 1000−1005.

(5) Galan, A.; Ballester, P. *Chem. Soc. Rev.* **2016**, *45*, 1720−1737.

(6) (a) Chen, J.; Rebek, J., Jr. *Org. Lett.* **2002**, *4*, 327−329. (b) Kaanumalle, L. S.; Ramamurthy, V. *Chem. Commun.* **2007**, 1062−1064. (c) Beyeh, N. K.; Puttreddy, R. *Dalton Trans.* **2015**, *44*, 9881−9886. (d) Gissot, A.; Rebek, J., Jr. *J. Am. Chem. Soc.* **2004**, *126*, 7424−7425.

(7) (a) Fujimoto, T.; Shimizu, C.; Hayashida, O.; Aoyama, Y. *Gazz. Chim. Ital.* **1997**, *127*, 749−752. (b) Hayashida, O.; Kato, M.; Akagi, K.; Aoyama, Y. *J. Am. Chem. Soc.* **1999**, *121*, 11597−11598. (c) Aoyama, Y.; Kanamori, T.; Nakai, T.; Sasaki, T.; Horiuchi, S.; Sando, S.; Niidome, T. *J. Am. Chem. Soc.* **2003**, *125*, 3455−3457. (d) Hayashida, O.; Mizuki, K.; Akagi, K.; Matsuo, A.; Kanamori, T.; Nakai, T.; Sando, S.; Aoyama, Y. *J. Am. Chem. Soc.* **2003**, *125*, 594−601.

(8) Iwanek, W.; Stefańska, K.; Szumna, A.; Wierzbicki, M. *RSC Adv.* **2016**, *6*, 13027−13031.

(9) (a) Nicolaou, K. C.; Snyder, S. A.; Montagnon, T.; Vassilikogiannakis, G. *Angew. Chem., Int. Ed.* **2002**, *41*, 1668−1698. (b) Kobayashi, S.; Jorgensen, K. A. In *Cycloaddition Reactions in Organic Synthesis*; Wiley-VCH Verlag GmbH: Weinheim, Germany, 2001. (c) Wenkert, E.; Piettre, S. R. *J. Org. Chem.* **1988**, *53*, 5850−5853. (d) Chen, C. H.; Rao, P. D.; Liao, C. C. *J. Am. Chem. Soc.* **1998**, *120*, 13254−13255. (e) Dyker, G.; Hildebrandt, D.; Liu, J.; Merz, K. *Angew. Chem., Int. Ed.* **2003**, *42*, 4399−4402. (f) Markgraf, J. H.; Patterson, D. E. *J. Heterocycl. Chem.* **1996**, *33*, 109−111.

(10) Paletta, M.; Klaes, M.; Neumann, B.; Stammler, H.-G.; Grimme, S.; Mattay, J. *Eur. J. Org. Chem.* **2008**, *2008*, 555−562.

(11) Zhao, J.-J.; Sun, S.-B.; He, S.-H.; Wu, Q.; Shi, F. *Angew. Chem., Int. Ed.* **2015**, *54*, 5460−5464.

(12) Sugimoto, H.; Nakamura, S.; Ohwada, T. *J. Org. Chem.* **2007**, *72*, 10088−10095.

(13) Weichert, A.; Hoffmann, H. M. R. *J. Org. Chem.* **1991**, *56*, 4098−4112.

(14) Frisch, M. J.; Trucks, G. W.; Schlegel, H. B.; Scuseria, G. E.; Robb, M. A.; Cheeseman, J. R.; Scalmani, G.; Barone, V.; Mennucci, B.; Petersson, G. A.; Nakatsuji, H.; Caricato, M.; Li, X.; Hratchian, H. P.; Izmaylov, A. F.; Bloino, J.; Zheng, G.; Sonnenberg, J. L.; Hada, M.; Ehara, M.; Toyota, K.; Fukuda, R.; Hasegawa, J.; Ishida, M.; Nakajima, T.; Honda, Y.; Kitao, O.; Nakai, H.; Vreven, T.; Montgomery, J. A., Jr.;

DOI: 10.1021/acs.joc.6b01099
J. Org. Chem. 2016, 81, 6018−6025

Peralta, J. E.; Ogliaro, F.; Bearpark, M.; Heyd, J. J.; Brothers, E.; Kudin, K. N.; Staroverov, V. N.; Kobayashi, R.; Normand, J.; Raghavachari, K.; Rendell, A.; Burant, J. C.; Iyengar, S. S.; Tomasi, J.; Cossi, M.; Rega, N.; Millam, J. M.; Klene, M.; Knox, J. E.; Cross, J. B.; Bakken, V.; Adamo, C.; Jaramillo, J.; Gomperts, R.; Stratmann, R. E.; Yazyev, O.; Austin, A. J.; Cammi, R.; Pomelli, C.; Ochterski, J. W.; Martin, R. L.; Morokuma, K.; Zakrzewski, V. G.; Voth, G. A.; Salvador, P.; Dannenberg, J. J.; Dapprich, S.; Daniels, A. D.; Farkas, Ö.; Foresman, J. B.; Ortiz, J. V.; Cioslowski, J.; Fox, D. J. *Gaussian 09*, revision D.01; Gaussian, Inc.: Wallingford, CT, 2009.

(15) Jensen, F. In *Introduction to Computational Chemistry*, 2nd ed.; John Wiley & Sons Ltd: Chichester, U.K., 2007.

(16) Reed, A. E.; Weinstock, R. B.; Weinhold, F. *J. Chem. Phys.* **1985**, *83*, 735−746.

(17) Mendoza Huizar, L. H.; Rios-Reyes, C. H.; Olvera-Maturano, N. J.; Robles, J.; Rodriguez, J. A. *Open Chem.* **2015**, *13*, 52−60.

(18) Jędrzejewska, H.; Kwit, M.; Szumna, A. *Chem. Commun.* **2015**, *51*, 13799−13801.

DOI: 10.1021/acs.joc.6b01099
J. Org. Chem. 2016, 81, 6018−6025